

Quantitative PCR Analysis of DNA, RNAs, and Proteins in the Same Single Cell

Anders Ståhlberg,^{1,2*} Christer Thomsen,¹ David Ruff,³ and Pierre Åman¹

BACKGROUND: The single cell represents the basic unit of all organisms. Most investigations have been performed on large cell populations, but understanding cell dynamics and heterogeneity requires single-cell analysis. Current methods for single-cell analysis generally can detect only one class of analytes.

METHODS: Reverse transcription and the proximity ligation assay were coupled with quantitative PCR and used to quantify any combination of DNA, mRNAs, microRNAs (miRNAs), noncoding RNAs (ncRNAs), and proteins from the same single cell. The method was used on transiently transfected human cells to determine the intracellular concentrations of plasmids, their transcribed mRNAs, translated proteins, and downstream RNA targets.

RESULTS: We developed a whole-cell lysis buffer to release unfractionated DNA, RNA, and proteins that would not degrade any detectable analyte or inhibit the assay. The dynamic range, analytical sensitivity, and specificity for quantifying DNA, mRNAs, miRNAs, ncRNAs, and proteins were shown to be accurate down to the single-cell level. Correlation studies revealed that the intracellular concentrations of plasmids and their transcribed mRNAs were correlated only moderately with translated protein concentrations (Spearman correlation coefficient, 0.37 and 0.31, respectively; $P < 0.01$). In addition, an ectopically expressed gene affected the correlations between analytes and this gene, which is related to gene regulation.

CONCLUSIONS: This method is compatible with most cell-sampling approaches, and generates output for the same parameter for all measured analytes, a feature facilitating comparative data analysis. This approach should open up new avenues in molecular diagnostics for detailed correlation studies of multi-

ple and different classes of analytes at the single-cell level.

© 2012 American Association for Clinical Chemistry

Cells of organs and tissues act in close connection with each other. Although they may be morphologically and genetically identical, cells may respond to stimuli in concert or individually. Studies have shown that individual cells exhibit distinct expression profiles of transcripts and proteins, even in seemingly homogeneous populations (1–3). Molecule numbers fluctuate in individual cells to produce unique responses to molecular cues that lead to distinct paths of development and cell differentiation (2, 3). Experimental work flows for characterizing cellular responses typically use large numbers of cells to reach the detection thresholds of analytical systems. Such experiments illuminate only the common behavior of cells in populations. New, analytically sensitive methods that can detect and quantify the few molecules present in single cells are needed for understanding the roles of individual cells and their interplay in tissues and organisms.

Recent reports have highlighted new approaches to surveying various analytes at the single-cell level in vivo, in situ, and in solution (4, 5). For example, reverse-transcription quantitative real-time PCR (RT-qPCR)⁴ has been successfully applied to measure mRNAs (6–11) and microRNAs (miRNAs) (12) at the single-cell level. Individual cells are usually collected by microaspiration (6, 7), flow cytometry (9, 10), or laser-capture microdissection (11, 13). The captured cells are then lysed and analyzed by RT-qPCR. The use of unfractionated lysates is advantageous for avoiding RNA losses (14). Analyses of many genes require pre-amplification to ensure that enough molecules are present in the reaction tube after sample dilution. Most

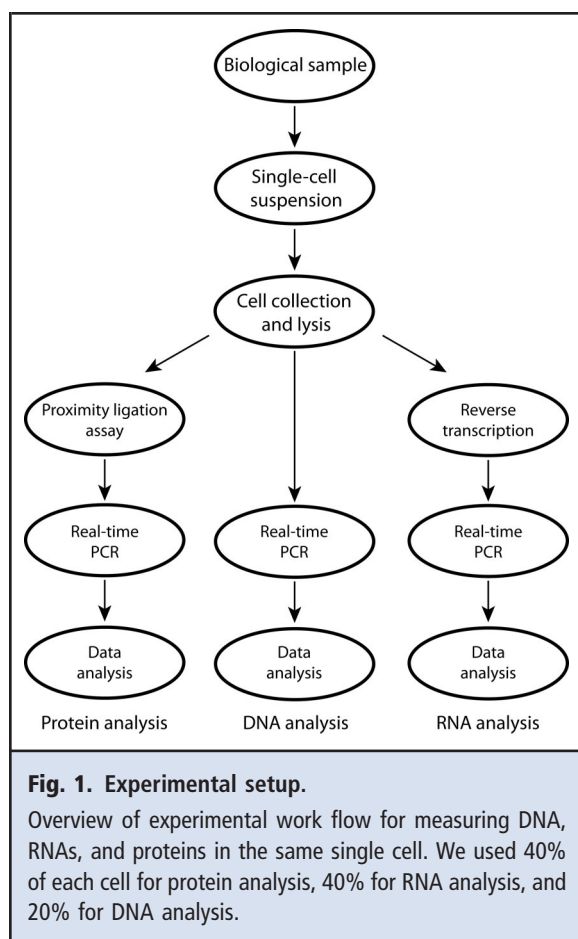
¹ Department of Pathology, Sahlgrenska Cancer Center, University of Gothenburg, Gothenburg, Sweden; ² TATAA Biocenter, Gothenburg, Sweden; ³ Applied Biosystems, Part of Life Technologies, Foster City, CA.

* Address correspondence to this author at: Sahlgrenska Cancer Center, Department of Pathology, University of Gothenburg, Box 425, SE-40530 Gothenburg, Sweden. Fax +46-31-828733; e-mail anders.stahlberg@gu.se.

Received June 19, 2012; accepted August 30, 2012.

Previously published online at DOI: 10.1373/clinchem.2012.191445

⁴ Nonstandard abbreviations: RT-qPCR, reverse-transcription quantitative real-time PCR; miRNA, microRNA; PLA, proximity ligation assay; PLA-qPCR, proximity ligation assay combined with quantitative real-time PCR; ncRNA, noncoding RNA; GFP, enhanced green fluorescent protein; FACS, fluorescence-activated cell sorting; AR, analyte-releasing; Cq, cycle of quantification.



preamplification protocols are compatible with RT-qPCR, but PCR-based preamplification protocols are usually preferred because they are easy to implement in the work flow, generate high yields, and are target specific. Furthermore, the use of qPCR and the proximity ligation assay (PLA) in combination (PLA-qPCR) is capable of quantifying proteins in cell lysates, but the method has not yet been applied to single cells (15). All of these work flows interrogate one class of molecule at a time, however. For a deeper understanding of complex biological processes, it is highly advantageous to measure multiple types of analytes in the same single cell.

We describe a method for quantifying DNA, mRNAs, miRNAs, noncoding RNAs (ncRNAs), and proteins with qPCR in the same cell (Fig. 1). By applying qPCR to measure all these classes of analytes, we have achieved a high analytical sensitivity and a large dynamic range and have eliminated the need to combine different technology platforms. The approach was used with transiently transfected human cells that ec-

topically express the *FUS*⁵ (fused in sarcoma) gene. *FUS* is a multifunctional protein that regulates gene activity through interacting with other proteins, RNAs, and DNA (16). Furthermore, *FUS* is implicated in the regulation of gene promoter activity (17), is involved in pre-mRNA splicing (18), and shuttles between the nucleus and the cytoplasm bound to RNA (19). The *CCND1* (cyclin D1) gene, which is involved in cell cycle regulation, is one well-characterized target gene of *FUS* (17). *FUS* is found in fusion oncogenes occurring in some sarcomas and leukemias (20). Recently, *FUS* mutations have also been implicated in familial forms of the neurodegenerative disorders amyotrophic lateral sclerosis and frontotemporal lobar degeneration (21, 22).

Materials and Methods

CELL CULTURES AND TRANSFECTIONS

The human fibrosarcoma cell line HT1080 was cultured at 37 °C with air containing 5% CO₂ and in RPMI 1640 GlutaMAX medium supplemented with 100 U/mL penicillin, 100 μg/mL streptomycin, and 100 mL/L fetal bovine serum (all from Life Technologies). HT1080 cells were seeded into 6-well plates (Nunc) at a density of 150 000 cells/well and transfected after 18–24 h. Each well was transfected with a mixture containing 1 μg of an expression plasmid encoding *FUS* tagged with enhanced green fluorescent protein (*FUS*-GFP) (23) and 3 μL FuGENE 6 transfection reagent (Roche) prepared in serum-free RPMI 1640 according to the manufacturer's instructions. Culture media were exchanged 6 h after transfection, and cells were harvested for analysis 24 h after transfection. The transfection efficiency was estimated at between 60% and 80% according to either fluorescence-activated cell sorting (FACS) analysis or visual inspection.

PROTEIN EXTRACTION AND IMMUNOBLOT ANALYSIS

Cells were washed with ice-cold PBS (PBS tablets, Life Technologies) and detached with a cell scraper into 100 μL/well of RIPA buffer (50 mmol/L Tris-HCl, pH 8.0, 150 mmol/L NaCl, 10 mL/L IGEPAL® CA-630, 5 g/L sodium deoxycholate, 1 g/L SDS; all from Sigma-Aldrich) supplemented with 1× Halt Protease and Phosphatase Inhibitor Cocktail (Thermo Scientific). Samples were incubated on ice for 10 min and cleared by centrifugation at 14 000g for 10 min at 4 °C. Immunoblotting was performed with the NuPAGE Novex

⁵ Human genes: *FUS*, fused in sarcoma; *GAPDH*, glyceraldehyde 3 phosphate dehydrogenase; *CCND1*, cyclin D1; *MIR31*, microRNA 31; *SNORD48*, small nucleolar RNA, C/D box 48.

4%–12% Bis-Tris gel system (Life Technologies) according to the manufacturer's recommendations. In brief, protein extracts were mixed with NuPAGE LDS Sample Buffer and NuPAGE Sample Reducing Agent, denatured at 70 °C for 10 min, separated on NuPAGE 4%–12% Bis-Tris gels, and transferred to Invitrolon polyvinylidene difluoride membranes (Life Technologies) by wet blot. The membranes were blocked with either 50 g/L skim milk (Merck Chemicals) (for analysis of FUS and GFP) or 50 g/L BSA (Sigma-Aldrich) [for analysis of glyceraldehyde 3-phosphate dehydrogenase (*GAPDH*)] prepared in TBS-T buffer (50 mmol/L Tris-HCl, pH 6.8, 50 mmol/L NaCl, 0.5 mL/L Tween 20; all from Sigma-Aldrich). The membranes were then incubated for 90 min with 0.4 µg/mL anti-FUS antibody [FUS/TLS Antibody (4H11); Santa Cruz Biotechnology], 0.5 µg/mL anti-GFP antibody [Living Colors® A.v. Monoclonal Antibody (JL-8); Clontech], or 1 µg/mL anti-GAPDH antibody [Anti-GAPDH Antibody (mAbcam 9484) – Loading Control; Abcam]. Incubation with a peroxidase-conjugated goat antimouse antibody [Stabilized Goat Anti-Mouse IgG (H+L), Peroxidase Conjugated; Thermo-Scientific] followed by SuperSignal West Dura Extended Duration Substrate (Thermo Scientific) was used to detect protein bands. An LAS-4000 imaging system (Fujifilm) was used to capture the luminescence signals.

SINGLE-CELL ISOLATION

HT1080 cells were dissociated with RPMI 1640 GlutaMAX medium containing 2.5 g/L trypsin (both from Life Technologies) and 0.5 mmol/L EDTA (Merck Chemicals). Trypsin was inactivated with cell medium containing fetal bovine serum. Dissociated cells were washed once with and then kept in cell medium containing 20 mL/L fetal bovine serum. Cell aggregates were removed by filtering with a 70-µm cell strainer (BD Biosciences). We used a BD FACSAria 2 cell sorter (BD Biosciences) to sort single cells into 96-well PCR plates (Life Technologies) containing 5 µL analyte-releasing (AR) lysis buffer (Life Technologies). AR lysis buffer is a buffered hypotonic lysis reagent of low ionic strength (1 g/L nondetergent sulfobetaine 201, 50 mmol/L Tris-HCl, pH 8.0, and 1 mmol/L EDTA, pH 8.0) mixed 1:1 with PBS (PBS Tablets; Life Technologies). Samples were frozen on dry ice and kept at –80 °C until subsequent analysis. A detailed protocol for single-cell sorting has been described elsewhere (24). We used 40% of the lysed cell—equivalent to 2 µL—for RT-qPCR, 40% for PLA-qPCR, and the remaining 20% for genomic DNA quantification with RT-qPCR. The PLA, reverse transcription, and qPCR for genomic DNA were run simultaneously in parallel reaction plates.

QIashredder kits (Qiagen) were used to homogenize lysates, and total RNA was isolated with an Exiqon

kit (miRCURY RNA Isolation Kit - Cell and Plant). Total RNA was measured with a NanoDrop ND-1000 spectrophotometer (NanoDrop Technologies).

PROXIMITY LIGATION ASSAYS

The FUS-GFP PLA proximity probes were constructed with rabbit prebiotinylated polyclonal anti-GFP antibodies [Anti-GFP Antibody (Biotin); Abcam], according to the manufacturer's instructions (TaqMan® Protein Assays Oligo Probe Kit; Life Technologies). In brief, the GFP PLA proximity probes were prepared by mixing 5 µL GFP biotinylated antibody (200 nmol/L) with 5 µL of either 3'-free end or 5'-free end streptavidin-conjugated oligonucleotide (200 nmol/L) in 2 separate 200-µL plastic tubes. After allowing complete biotin-streptavidin binding by incubation at ambient temperature for 60 min, the mix was diluted with 90 µL of PLA Probe Storage Buffer to make each 10-nmol/L PLA probe storage stock. Immediately before commencing the PLA reaction, both 3'-free end and 5'-free end PLA proximity probes were combined together and diluted 130 times in PLA Probe Dilution Buffer to make a 77-pmol/L 2× working probe solution. The optimal concentration of the working probe was obtained by titration (see Fig. 1 in the Data Supplement that accompanies the online version of this article at <http://www.clinchem.org/content/vol58/issue12>). The PLA was performed according to the manufacturers' instructions (TaqMan® Protein Assays Core Reagents Kit with Master Mix, Life Technologies). First, 2 µL PLA working probe solution was mixed with 2 µL lysed single cells and incubated at 37 °C for 60 min. We then added the ligation reaction mix to a final volume of 50 µL and incubated at 37 °C for 10 min. The ligation reaction mix contained 1× Ligation Reaction Buffer and 1× DNA Ligase. DNA Ligase was freshly diluted with ligase dilution buffer from a 500× long-term storage stock solution to a 1× working solution. Finally, 1× Protease solution was added to terminate the ligation reaction. The temperature profile for ligase inactivation was 37 °C for 10 min and 95 °C for 5 min. Samples were kept cold (4 °C–8 °C) between all incubation steps, and all subsequent steps were performed immediately. Background ligation was measured in AR lysis buffer controls containing no protein. PLA-qPCR specificity (Fig. 2) was checked with untransfected control cells lacking the FUS-GFP protein. Serial dilutions of a cell lysate containing FUS-GFP protein were used to generate a calibration curve for the PLA assay (see Fig. 2 in the online Data Supplement). The relative lysis efficiency for protein measurements was evaluated by measuring the same amount of protein lysed in either AR lysis buffer or standard PLA cell lysis buffer supplemented

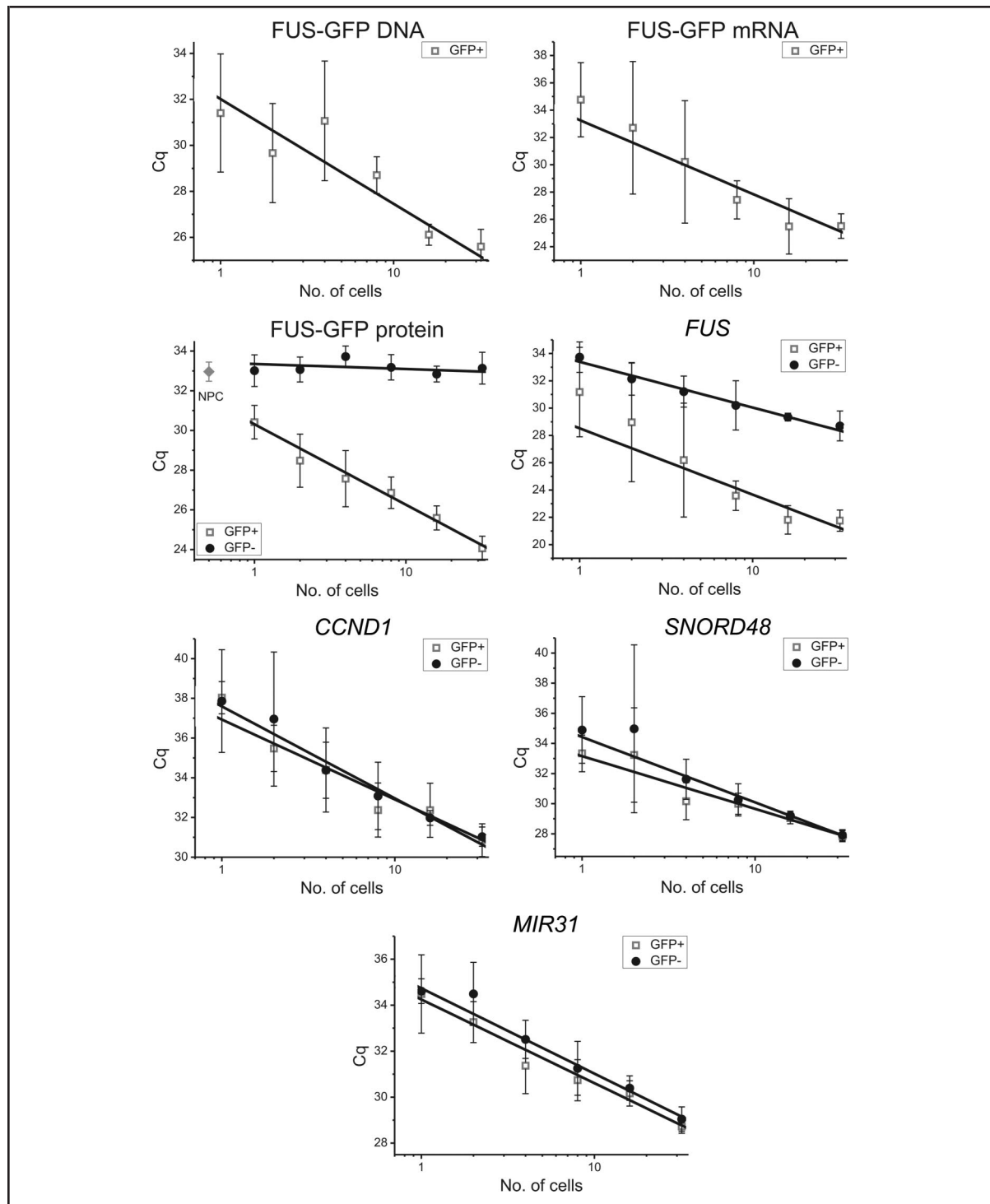


Fig. 2. Assay performance.

Analytical sensitivity and dynamic range for measuring 32 cells down to a single cell. GFP-fluorescent HT1080 cells transiently transfected with FUS-GFP-encoding plasmid (GFP+, open squares) and untransfected control cells without any FUS-GFP (GFP-, closed circles) were collected with FACS, and data were fitted by linear regression. The background signal from unspecific PLA probe binding was determined with negative protein controls (NPC, gray diamond). Data are plotted as the mean and SD ($n = 6$). FUS-GFP DNA indicates FUS-GFP-encoding DNA; FUS-GFP RNA indicates FUS-GFP-encoding RNA.

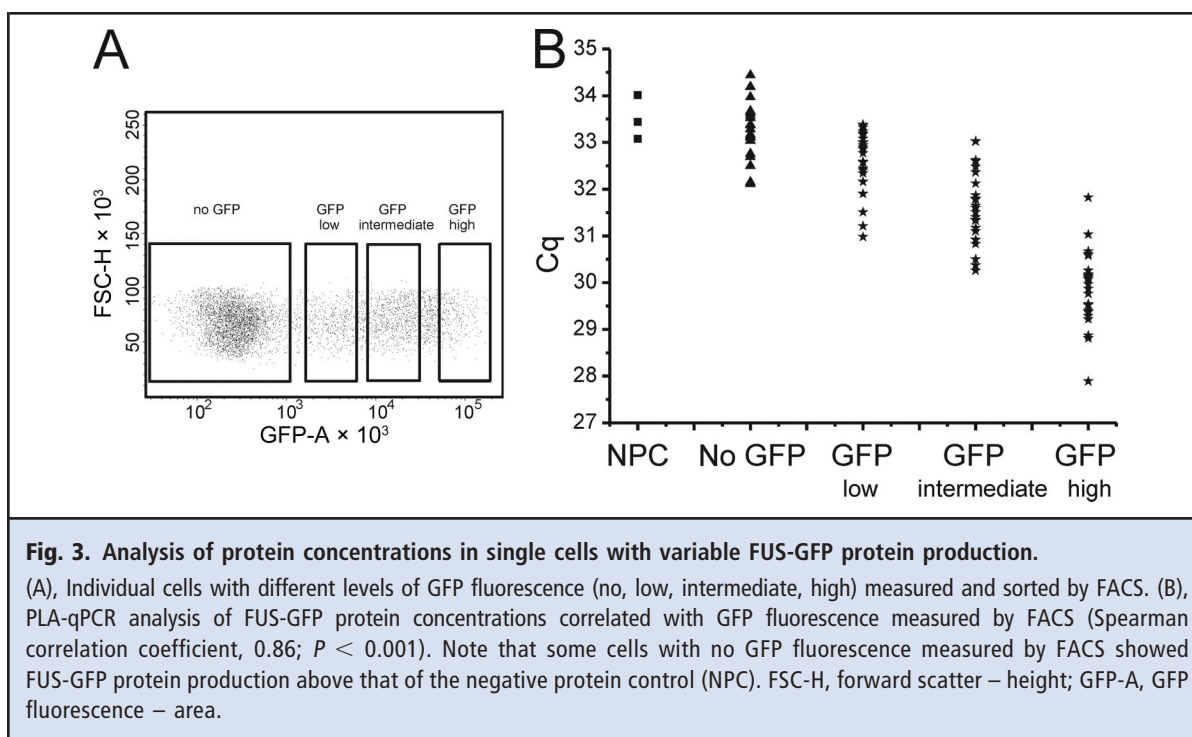


Fig. 3. Analysis of protein concentrations in single cells with variable FUS-GFP protein production.

(A), Individual cells with different levels of GFP fluorescence (no, low, intermediate, high) measured and sorted by FACS. (B), PLA-qPCR analysis of FUS-GFP protein concentrations correlated with GFP fluorescence measured by FACS (Spearman correlation coefficient, 0.86; $P < 0.001$). Note that some cells with no GFP fluorescence measured by FACS showed FUS-GFP protein production above that of the negative protein control (NPC). FSC-H, forward scatter – height; GFP-A, GFP fluorescence – area.

with 1× Halt Protease and Phosphatase Inhibitor Cocktail (see Fig. 3A in the online Data Supplement).

REVERSE TRANSCRIPTION

SuperScript® III Reverse Transcriptase (Life Technologies) was used for reverse transcription according to the manufacturers' instructions. Aliquots from lysed single cells (2 μ L) were incubated with 5 μ L water containing 0.5 mmol/L dNTP (deoxynucleoside triphosphate) mix (Sigma-Aldrich), 2.5 μ mol/L Oligo(dT)₁₂₋₁₈ Primer (Life Technologies), 2.5 μ mol/L random hexamers, and 0.5× reverse-transcription specific primer for *MIR31* (microRNA 31) (TaqMan MicroRNA Assay, 002279) and *SNORD48* (small nucleolar RNA, C/D box 48) (TaqMan MicroRNA Assay, 001006). Each reaction was performed at 65 °C for 5 min. We then added 50 mmol/L Tris-HCl (pH 8.3), 75 mmol/L KCl, 3 mmol/L MgCl₂, 5 mmol/L dithiothreitol, 10 U RNaseOut, and 50 U SuperScript III to a total volume of 10 μ L (all reagents from Life Technologies). Reverse transcription was performed with a temperature/time profile of 16 °C for 5 min, 50 °C for 60 min, 55 °C for 15 min, and a final heating step at 70 °C for 15 min. All samples were diluted to 20 μ L with water before the qPCR.

QUANTITATIVE REAL-TIME PCR

The Applied Biosystems 7500 Fast Real-Time PCR System (Life Technologies) was used for all real-time PCR

measurements. All RT-qPCR experiments were conducted so as to obtain at least the minimum information required for publication of quantitative real-time PCR experiments (25). For cDNA analysis, each reaction (10 μ L) contained TaqMan Fast Universal PCR Master Mix, either 1× TaqMan Gene Expression Assay or 1× TaqMan MicroRNA Assay (all from Life Technologies), and 2 μ L diluted cDNA. DNA and cDNA expression profiling of the sequences encoding FUS-GFP were performed with a custom-designed TaqMan assay (for details of these assays, see Table 1 in the online Data Supplement). The qPCR performed after the PLA contained TaqMan Protein Assay Fast Master Mix, 1× Universal PCR Assay (all from Life Technologies), and 9 μ L PLA template in a total volume of 20 μ L. The temperature profile for all assays was 95 °C for 20 s followed by 50 amplification cycles of 95 °C for 3 s and 60 °C for 30 s. Formation of PCR products of the correct lengths was confirmed by agarose gel electrophoresis. Assay performance was checked with calibration curves for all assays. Determination of values for the cycle of quantification (Cq) was performed with standard threshold lines. Analysis of single-cell data was performed as described elsewhere (9, 14, 24).

DATA ANALYSIS

FACS data were analyzed with FACSDIVA software (BD Biosciences). Untransfected control cells without FUS-GFP were used to gate “no GFP” (see Fig. 3A).

Note that some of these cells expressed FUS-GFP–encoding DNA and mRNA (see Table 2 in the online Data Supplement). Statistical analysis was performed with GenEx (MultiD Analyses), SPSS 19 (IBM/SPSS), and OriginPro 7.5 (OriginLab Corporation) software. Approximate differences in relative expression between mRNA and DNA encoding FUS-GFP, and between endogenous FUS-encoding mRNA and ectopic FUS-GFP–encoding mRNA, were calculated from data in Fig. 2. These calculations included corrections for all dilution steps.

Results

Transient transfection in the human fibrosarcoma cell line HT1080 was used to ectopically express FUS-GFP. The concentrations of FUS-GFP and endogenous FUS protein were of magnitudes similar to those obtained with immunoblot analysis at the cell population level (see Fig. 4 in the online Data Supplement). We quantified the number of transfected plasmids (FUS-GFP–encoding DNA), transcribed mRNAs (FUS-GFP–encoding mRNAs) and translated FUS-GFP protein in individual cells. The PLA-qPCR assay targeted the ectopically produced GFP-tagged protein, but not endogenously expressed FUS protein. In addition, cyclin D1 (*CCND1*) mRNA, small nucleolar RNA, C/D box 48 (*SNORD48*), and miRNA 31 (*MIR31*) were measured at the single-cell level. We chose to include *SNORD48* and *MIR31* in our experimental setup because *SNORD48* (ncRNA) and *MIR31* (miRNA) encode types of RNA molecules besides mRNA. In addition, the expression of these genes was correlated with *FUS* mRNA at the single-cell level (see below).

DEVELOPMENT OF A COMMON PURIFICATION-FREE PROTOCOL FOR DNA, RNA, AND PROTEIN ANALYSIS OF SINGLE CELLS

Single HT1080 cells were sorted by FACS, lysed in AR lysis buffer, and split into parallel work flows to facilitate specific analysis of DNA, RNA, and protein molecules with qPCR, RT-qPCR, and PLA-qPCR, respectively (Fig. 1). To minimize the loss of analytes during the experimental process, we used a whole-cell lysis procedure to prepare unfractionated RNA, DNA, and protein templates from individual cells. The applied AR lysis buffer is a hypotonic buffer of low ionic strength that efficiently lyses the cell, maintains DNA, RNA, and protein integrity without noticeable degradation, and is compatible with downstream enzymatic reactions without any detectable inhibition (see Figs. 3 and 5 in the online Data Supplement). The performance of the AR lysis buffer was compared at the cell population level with the performances of standard lysis buffers for RNA and protein preparation. The ncRNA (*SNORD48*) molecules are localized in the nu-

clei, whereas processed miRNA 31 (*MIR31*) molecules are localized in the cytoplasm; both were released equally compared with the control lysis, indicating that both compartments were efficiently lysed with the AR lysis buffer (see Fig. 3 in the online Data Supplement).

DNA, RNA, AND PROTEIN QUANTIFICATION AT THE SINGLE-CELL LEVEL

To evaluate the analytical sensitivity and dynamic range of all assays, we performed a calibration based on analyzing the material obtained from 32 FACS-sorted cells down to a single FACS-sorted cell collected in steps of 2 (Fig. 2). All assays were able to detect their respective target molecules at the single-cell level. The measured parameter, Cq, which is inversely proportional to the number of molecules on the log₂ scale, was linearly correlated with the logarithm of the number of analyzed cells. The observed variation in number of molecules increased as the number of analyzed cells decreased (Fig. 2). By comparing the variation among single cells to calibration curves generated from dilution series for the respective analytes (see Fig. 2 in the online Data Supplement), we found the biological variation to be higher than the technical variation for all assays (Fig. 2; see Tables 2 and 3 in the online Data Supplement). These results are in agreement with those described in our previous report (14), which showed that the biological cell-to-cell variation is substantially larger than the technical noise produced when quantifying low mRNA amounts with RT-qPCR.

Next, we showed that PLA-qPCR can be accurately applied to quantify proteins in individual cells (Fig. 2). In contrast to qPCR measurements of DNA and RNA, protein measurements with PLA-qPCR produce background signals. For the FUS-GFP PLA-qPCR assay, we inferred that the background signal was due to unspecific ligation between the 2 PLA probes, because the signal of the controls with no protein was indistinguishable from that of cell lysates without FUS-GFP protein (Fig. 2). The analytical sensitivity of PLA-qPCR to detect and quantify FUS-GFP protein molecules at low concentrations was dependent on the PLA probe concentration (see Fig. 1 in the online Data Supplement). Reducing the concentration of the PLA probe increased the analytical sensitivity to allow measurement of a few FUS-GFP protein molecules, but this sensitivity came at the expense of precision when large numbers of FUS-GFP protein molecules were measured.

The DNA in the plasmid encoding FUS-GFP and the cDNA generated from FUS-GFP–encoding mRNA are identical in sequence. To allow specific quantification of the DNA and mRNA encoding FUS-GFP, we split the single-cell samples before cDNA synthesis for the respective DNA and RNA analyses (Fig. 1). The

Table 1. Spearman correlations between all analytes for all single cells with increasing GFP fluorescence intensity.^a

	FUS-GFP protein	FUS-GFP DNA ^b	FUS-GFP mRNA	FUS DNA/RNA	CCND1 mRNA	MIR31 miRNA	SNORD48 ncRNA
FUS-GFP Protein	1						
FUS-GFP DNA	0.37**	1					
FUS-GFP mRNA	0.31**	0.41**	1				
FUS DNA/RNA	0.36**	0.44**	0.92**	1			
CCND1 mRNA	-0.11	-0.29*	-0.16	0.10	1		
MIR31 miRNA	-0.10	-0.11	0.02	0.17	0.59**	1	
SNORD48 ncRNA	-0.10	-0.21	0.07	0.24*	0.71**	0.66**	1

^a Statistically significant ($P < 0.01$, and $P < 0.05$) Spearman correlation coefficients are marked (** and *, respectively). Distributions and statistical parameters for all analytes are shown in Fig. 6 and Table 1 in the online Data Supplement. Numbers of single cells analyzed were as follows: $n_{\text{no GFP}} = 24$; $n_{\text{GFP high}} = 24$; $n_{\text{GFP intermediate}} = 24$; $n_{\text{GFP low}} = 19$; and $n_{\text{NPC}} = 3$. NPC, negative protein control.

^b FUS-GFP DNA indicates FUS-GFP–encoding DNA; FUS-GFP RNA indicates FUS-GFP–encoding RNA.

amount of FUS-GFP–encoding mRNA was about 5 times higher than that for FUS-GFP–encoding DNA (Fig. 2). Hence, the majority of the measured cDNA molecules encoding FUS-GFP originated from mRNA and was not plasmid DNA. The *FUS* assay targeted the total amount of FUS-GFP–encoding DNA, FUS-GFP–encoding mRNA, and endogenously expressed *FUS*. The fact that the *FUS* assay produced a fluorescence signal in cells producing FUS-GFP that was 10 times higher than that in control cells demonstrated that most molecules originated from the transiently expressed plasmid (Fig. 2).

STUDIES OF CORRELATIONS AMONG DIFFERENT ANALYTES AT THE SINGLE-CELL LEVEL

The capacity to quantify several different analytes in single cells opens up possibilities to study interaction networks in detail. To study such correlations, we transiently transfected HT1080 cells with FUS-GFP–encoding plasmid and collected single cells with increasing GFP fluorescence intensity as measured by FACS.

Fluorescence intensity is expected to be linearly proportional to the number of fluorescent molecules. We confirmed this relationship by correlating the increasing GFP FACS fluorescence intensity to the number of FUS-GFP protein molecules measured by PLA-qPCR (Spearman correlation coefficient, 0.86; $P < 0.01$) (Fig. 3). This high correlation coefficient indicates that the majority of FUS-GFP protein molecules were available for PLA-qPCR analysis.

The same single cells were also analyzed for the other analytes (see Fig. 6 and Table 2 in the online Data Supplement). As expected, the concentrations of FUS-GFP protein, FUS-GFP–encoding DNA, and FUS-

GFP–encoding mRNA were all correlated within individual cells (Table 1; Spearman correlations with P values < 0.01), but large variation was observed among individual cells (see Fig. 6 and Table 2 in the online Data Supplement). The distributions of FUS-GFP–encoding DNA and FUS-GFP–encoding mRNA were wide, spanning 4 orders of magnitude, and the distribution of FUS-GFP protein spanned 2 orders of magnitude. The observed correlation between FUS-GFP–encoding DNA and FUS-GFP protein (Spearman correlation, 0.37; $P < 0.01$) demonstrated that a high intracellular plasmid concentration was favorable for protein production but was not the sole parameter determining successful plasmid-to-protein translation. The observed variation in transcription and translation efficiencies could be due to plasmid aggregation and to cell-to-cell heterogeneity caused by such factors as local microenvironment, cell size, cell density, and cell cycle state (26, 27). Transcription and translation occur in bursts, which result in variation over time (28–30). The time scales are minutes to hours for transcriptional pulsing (30–32) and hours to days for translational pulsing (1, 33), but different molecules vary greatly with respect to these times. Mathematical modeling and experimental data have shown that the variation in RNA and protein among individual cells at a given time point fit with the observed variation in RNA and protein over time (1, 32). Our data are in agreement with these reports.

The expression measured with the *FUS* assay, which targeted endogenous *FUS*, FUS-GFP–encoding DNA, and FUS-GFP–encoding mRNA, correlated moderately with the amounts of FUS-GFP–encoding DNA (Spearman correlation coefficient, 0.44; $P < 0.01$) and FUS-GFP protein (Spearman correlation co-

efficient, 0.36; $P < 0.01$), and this expression correlated strongly with the expression of FUS-GFP–encoding mRNA (Spearman correlation coefficient, 0.92; $P < 0.01$), confirming that most target molecules of the *FUS* assay originated from the cDNA of the transiently expressed plasmids and not from the endogenous *FUS* gene (Fig. 2).

ECTOPIC GENE EXPRESSION MODULATES ANALYTE CORRELATIONS

To study cell population heterogeneity and correlations between analytes, we collected single cells randomly, regardless of their GFP fluorescence. The effect of ectopic *FUS* expression was evaluated by comparing FUS-GFP protein–positive cells and FUS-GFP protein–negative cells. A cell was considered FUS-GFP protein positive if its signal was significantly greater than the PLA-qPCR background signal (i.e., $P < 0.05$; see Fig. 7 and Table 3 in the online Data Supplement). We found that the expression levels of *FUS*, *CCND1*, *MIR31*, and *SNORD48* were all correlated in cells without ectopic *FUS* (Spearman correlations coefficients >0.66 ; $P < 0.01$) (Fig. 4A; see Table 4A in the online Data Supplement). In contrast, cells with ectopic *FUS* expression showed decreased or no correlations between *FUS* and *MIR31*, *CCND1*, or *SNORD48* (Fig. 4B; see Table 4 in the online Data Supplement). This observation can be explained by the fact that plasmid transcription is driven by a cytomegalovirus promoter and not by the endogenous *FUS* promoter (see Fig. 8 in the online Data Supplement). Consequently, the correlations of *FUS* to *MIR31*, *CCND1*, and *SNORD48* were lost in FUS-GFP protein–producing cells, because most *FUS* mRNAs originated from the plasmid. The observed changes in correlation values for ectopic *FUS* (while the other correlations between *MIR31*, *CCND1*, and *SNORD48* were unaffected) also indicated that our applied whole-cell lysis was reproducible and uniform. The existence of variation in cell lysis efficiency would be expected to generate systematic bias in correlations, not a specific change for a given, manipulated correlation.

Discussion

Several high-resolution analytical methods capable of detecting, visualizing, and quantifying analytes at the single-cell level have been reported (4, 5). Few of these methods can be used in combination or to measure multiple classes of biomolecules in the same single cell, however. FACS analysis is one successfully applied method that has been used to analyze single cells with a high throughput (3, 4, 34–36). Approximately 18 different proteins can be analyzed simultaneously in a FACS instrument. In addition, DNA-binding dyes can

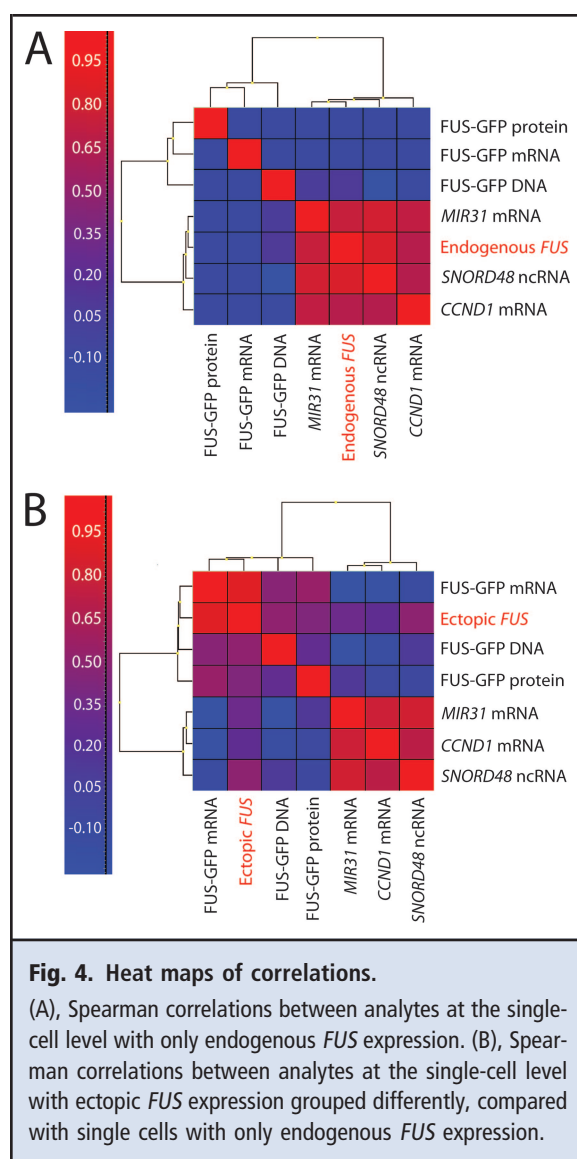


Fig. 4. Heat maps of correlations.

(A), Spearman correlations between analytes at the single-cell level with only endogenous *FUS* expression. (B), Spearman correlations between analytes at the single-cell level with ectopic *FUS* expression grouped differently, compared with single cells with only endogenous *FUS* expression.

be used to quantify nucleic acids in combination with proteins (4, 37).

We have demonstrated how individual cells can be efficiently lysed with a whole-cell lysis buffer that is also compatible with downstream enzymatic reactions used to measure DNA, mRNAs, miRNAs, ncRNAs, and proteins. The method is also compatible with most single-cell collection methods, including FACS, which also allows several additional markers to be analyzed at the single-cell level (4, 34–36). The described approach requires only a standard real-time PCR instrument, and all measurements generate output for the same parameter (Cq), which facilitates comparative data analysis. PLA and reverse transcription are run in separate tubes because of their different optimal reaction conditions,

a fact that precludes multiplexing between proteins and RNAs. In addition, the PLA reaction requires substantial dilution after the initial PLA probe targeting the protein-binding step in order to reduce background ligation events. The use of qPCR allows both short and long RNA sequences to be measured, whereas most other techniques cannot analyze short RNAs. In principle, the entire transcriptome can be analyzed by applying preamplification techniques, and up to 24 proteins have been successfully measured via multiplex PLA (38). It may also be possible to integrate microfluidics devices into the method we have described for quantifying DNA, RNAs, and proteins with qPCR and PLA (39). The described approach offers new possibilities for unifying genomic and proteomic investigations. The ability to quantify and correlate different classes of analytes in the same single cell may open up avenues in cell biology and molecular diagnostics.

Author Contributions: All authors confirmed they have contributed to the intellectual content of this paper and have met the following 3 re-

quirements: (a) significant contributions to the conception and design, acquisition of data, or analysis and interpretation of data; (b) drafting or revising the article for intellectual content; and (c) final approval of the published article.

Authors' Disclosures or Potential Conflicts of Interest: Upon manuscript submission, all authors completed the author disclosure form. Disclosures and/or potential conflicts of interest:

Employment or Leadership: D. Ruff, Life Technologies.

Consultant or Advisory Role: A. Ståhlberg, TATAA Biocenter.

Stock Ownership: A. Ståhlberg, TATAA Biocenter; D. Ruff, Life Technologies.

Honoraria: None declared.

Research Funding: A. Ståhlberg, Swedish Research Council (2367), Swedish Society for Medical Research, Johan Jansson Foundation for Cancer Research, Assar Gabrielssons Research Foundation, and Wilhelm and Martina Lundgren Foundation for Scientific Research; P. Åman, Swedish Cancer Society.

Expert Testimony: None declared.

Patents: D. Ruff, United States patent US 8,012,685.

Role of Sponsor: The funding organizations played no role in the design of study, choice of enrolled patients, review and interpretation of data, or preparation or approval of manuscript.

Acknowledgments: We thank M. Bengtsson, M. Hemberg, and M. Kubista for critical reading of the manuscript.

References

1. Raj A, Peskin CS, Tranchina D, Vargas DY, Tyagi S. Stochastic mRNA synthesis in mammalian cells. *PLoS Biol* 2006;4:e309.
2. Raj A, Rifkin SA, Andersen E, van Oudenaarden A. Variability in gene expression underlies incomplete penetrance. *Nature* 2010;463:913–8.
3. Chang HH, Hemberg M, Barahona M, Ingber DE, Huang S. Transcriptome-wide noise controls lineage choice in mammalian progenitor cells. *Nature* 2008;453:544–7.
4. Kalisky T, Blainey P, Quake SR. Genomic analysis at the single-cell level. *Annu Rev Genet* 2011;45:431–5.
5. Wu M, Singh AK. Single-cell protein analysis. *Curr Opin Biotechnol* 2012;23:83–8.
6. Bengtsson M, Ståhlberg A, Rorsman P, Kubista M. Gene expression profiling in single cells from the pancreatic islets of Langerhans reveals log-normal distribution of mRNA levels. *Genome Res* 2005;15:1388–92.
7. Liss B, Franz O, Sewing S, Bruns R, Neuhoff H, Roeper J. Tuning pacemaker frequency of individual dopaminergic neurons by Kv4.3L and KChip3.1 transcription. *EMBO J* 2001;20:5715–24.
8. Reiter M, Kirchner B, Muller H, Holzhauser C, Mann W, Pfaffl MW. Quantification noise in single-cell experiments. *Nucleic Acids Res* 2011;39:e124.
9. Ståhlberg A, Andersson D, Aurelius J, Faiz M, Pekna M, Kubista M, Pekny M. Defining cell populations with single-cell gene expression profiling: correlations and identification of astrocyte subpopulations. *Nucleic Acids Res* 2011;39:e24.
10. Warren L, Bryder D, Weissman IL, Quake SR. Transcription factor profiling in individual hematopoietic progenitors by digital RT-PCR. *Proc Natl Acad Sci U S A* 2006;103:17807–12.
11. Gründemann J, Schlaudraff F, Haeckel O, Liss B. Elevated α -synuclein mRNA levels in individual UV-laser-microdissected dopaminergic substantia nigra neurons in idiopathic Parkinson's disease. *Nucleic Acids Res* 2008;36:e38.
12. Tang F, Hajkova P, Barton SC, Lao K, Surani MA. MicroRNA expression profiling of single whole embryonic stem cells. *Nucleic Acids Res* 2006;32:e9.
13. Kamme F, Salunga R, Yu J, Tran DT, Zhu J, Bittner A, et al. Single-cell microarray analysis in hippocampus CA1: demonstration and validation of cellular heterogeneity. *J Neurosci* 2003;23:3607–15.
14. Bengtsson M, Hemberg M, Rorsman P, Ståhlberg A. Quantification of mRNA in single cells and modeling of RT-qPCR induced noise. *BMC Mol Biol* 2008;9:63.
15. Fredriksson S, Gullberg M, Jarvis J, Olsson C, Pietras K, Gustafsdottir SM, et al. Protein detection using proximity-dependent DNA ligation assays. *Nat Biotechnol* 2002;20:473–7.
16. Tan AY, Manley JL. The TET family of proteins: functions and roles in disease. *J Mol Cell Biol* 2009;1:82–92.
17. Wang X, Arai S, Song X, Reichart D, Du K, Pascual G, et al. Induced ncRNAs allosterically modify RNA-binding proteins in cis to inhibit transcription. *Nature* 2008;454:126–30.
18. Yang L, Embree LJ, Tsai S, Hickstein DD. Onco-protein TLS interacts with serine-arginine proteins involved in RNA splicing. *J Biol Chem* 1998;273:27761–4.
19. Zinszner JH, Sok J, Immanuel D, Yin Y, Ron D. TLS (FUS) binds RNA in vivo and engages in nucleocytoplasmic shuttling. *J Cell Sci* 1997;110:1741–50.
20. Riggi N, Cironi L, Suva ML, Stamenkovic I. Sarcomas: genetics, signalling, and cellular origins. Part 1: the fellowship of TET. *J Pathol* 2007;213:4–20.
21. Kwiatkowski TJ Jr, Bosco DA, Leclerc AL, Tamrazian E, Vandenberg CR, Russ C, et al. Mutations in the FUS/TLS gene on chromosome 16 cause familial amyotrophic lateral sclerosis. *Science* 2009;323:1205–8.
22. Lagier-Tourenne C, Polymenidou M, Cleveland DW. TDP-43 and FUS/TLS: emerging roles in RNA processing and neurodegeneration. *Hum Mol Genet* 2010;19:R46–64.
23. Thelin-Järnum S, Göransson M, Burguete AS, Olofsson A, Åman P. The myxoid liposarcoma specific TLS-CHOP fusion protein localizes to nuclear structures distinct from PML nuclear bodies. *Int J Cancer* 2002;97:446–50.
24. Ståhlberg A, Bengtsson M. Single-cell gene expression profiling using reverse transcription quantitative real-time PCR. *Methods* 2010;50:282–8.
25. Bustin SA, Benes V, Garson J, Hellemans J, Huggett J, Kubista M, et al. The MIQE guidelines: minimum information for publication of quantitative real-time PCR experiments. *Clin Chem* 2009;55:611–22.
26. Snijder B, Pelkman L. Origins of regulated cell-to-cell variability. *Nat Rev Mol Cell Biol* 2011;12:119–25.
27. Snijder B, Sacher R, Rämö P, Damm EM, Liberali P, Pelkmans L. Population context determines cell-to-cell variability in endocytosis and virus infection. *Nature* 2009;461:520–3.
28. Raj A, van Oudenaarden A. Nature, nurture or

- chance: stochastic gene expression and its consequences. *Cell* 2008;135:216–26.
29. Yu J, Xiao J, Ren X, Lao K, Xie XS. Probing gene expression in live cells, one protein molecule at a time. *Science* 2006;311:1600–3.
 30. Chubb JR, Trcek T, Shenoy SM, Singer RH. Transcriptional pulsing of a developmental gene. *Current Biol* 2006;16:1018–25.
 31. Yunger S, Rosenfeld L, Garini Y, Shav-Tal Y. Single-allele analysis of transcription kinetics in living mammalian cells. *Nat Methods* 2010;7:631–3.
 32. Larson DR, Singer RH, Zenklusen D. A single molecule view of gene expression. *Trends Cell Biol* 2009;19:630–7.
 33. Sigal A, Milo R, Cohen A, Geva-Zatorsky N, Klein Y, Liron Y, et al. Variability and memory of protein levels in human cells. *Nature* 2006;444:643–6.
 34. Sachs K, Perez O, Pe'er D, Lauffenburger DA, Nolan GP. Causal protein-signaling networks derived from multiparameter single-cell data. *Science* 2005;308:523–9.
 35. Newman JR, Ghaemmaghami S, Ihmels J, Breslow DK, Noble M, DeRisi JL, et al. Single-cell proteomic analysis of *S. cerevisiae* reveals the architecture of biological noise. *Nature* 2006;441:840–6.
 36. Bar-Even A, Paulsson J, Maheshri N, Carmi M, O'Shea E, Pilpel Y, Barkai N. Noise in protein expression scales with natural protein abundance. *Nat Genet* 2006;38:636–43.
 37. Trask BJ, Mefford H, van den Engh G, Massa HF, Juyal RC, Potocki L, et al. Quantification by flow cytometry of chromosome-17 deletions in Smith-Magenis syndrome patients. *Hum Genet* 1996;98:710–8.
 38. Lundberg M, Thorsen SB, Assarsson E, Villablanca A, Tran B, Gee N, et al. Multiplexed homogeneous proximity ligation assays for high-throughput protein biomarker research in serological material. *Mol Cell Proteomics* 2011;10:M110.004978.
 39. White AK, VanInsberghe M, Petriv OI, Hamidi M, Sikorski D, Marra MA, et al. High-throughput microfluidic single-cell RT-qPCR. *Proc Natl Acad U S A* 2011;108:13999–4004.